

Effect of P-wave interaction in ${}^6\text{He}$ and ${}^6\text{Li}$ photoabsorption

Sonia Bacca^{1,2}, Nir Barnea³, Winfried Leidemann¹ and Giuseppina Orlandini¹

¹ *Dipartimento di Fisica, Università di Trento and INFN (Gruppo Collegato di Trento),
via Sommarive 14, I-38050 Povo, Italy*

² *Institut für Kernphysik, Johannes-Gutenberg Universität Mainz,
Johann-Joachim-Becher Weg 45, D-55099 Mainz, Germany and*

³ *Racah Institute of Physics, Hebrew University, 91904, Jerusalem, Israel*

(Dated: October 25, 2018)

Abstract

The total photoabsorption cross sections of the six-body nuclei are calculated including complete final state interaction via the Lorentz Integral Transform method. The effect of nucleon-nucleon central P-wave forces is investigated. Comparing to results with central potentials containing S-wave forces only, one finds considerably more strength in the low-energy cross sections and a rather strong improvement in comparison with experimental data, in particular for ${}^6\text{Li}$.

PACS numbers: 21.45.+v, 24.30.Cz, 25.20.Dc, 31.15.Ja

In a recent paper [1] we carried out the first microscopic calculation of total photoabsorption cross sections for $A = 6$ nuclei. Semi-realistic central S-wave forces were taken as NN interaction. The obtained cross sections were not in good agreement with the low-energy data. Since ${}^6\text{He}$ and ${}^6\text{Li}$ are P-shell nuclei we suspected in [1] that this observable could show a sensitivity to the P-wave NN interaction. The aim of the present work is to check this conjecture. To this end we use the recently published AV4' potential [3], which includes S- and P-waves forces.

Our calculation proceeds in the same way as in [1]. Here we summarize the main steps. The total photoabsorption cross section in unretarded dipole approximation is given by

$$\sigma(\omega) = 4\pi^2\alpha\omega R(\omega), \quad (1)$$

where α is the fine structure constant, ω the photon energy, and

$$R(\omega) = \int d\Psi_f \left| \langle \Psi_f | \hat{D}_z | \Psi_0 \rangle \right|^2 \delta(E_f - E_0 - \omega) \quad (2)$$

the response function; wave functions and energies of ground and final state are denoted by $|\Psi_{0/f}\rangle$ and $E_{0/f}$ respectively, while

$$\hat{D}_z = \sum_{i=1}^A \frac{\tau_i^3 z'_i}{2} \quad (3)$$

is the unretarded dipole operator. Here τ_i^3 and z'_i represent the third component of the isospin operator and of the spatial coordinate of the i -th particle in the center of mass frame, respectively. In the Lorentz Integral Transform (LIT) method [4] one obtains $R(\omega)$ from the inversion of an integral transform with a Lorentzian kernel

$$L(\sigma_R, \sigma_I) = \int d\omega \frac{R(\omega)}{(\omega - \sigma_R)^2 + \sigma_I^2} = \langle \tilde{\Psi} | \tilde{\Psi} \rangle, \quad (4)$$

where the "Lorentz state" $\tilde{\Psi}$ is the unique solution of an inhomogeneous "Schrödinger-like" equation

$$(H - E_0 - \sigma_R + i\sigma_I)|\tilde{\Psi}\rangle = \hat{D}_z|\Psi_0\rangle \quad (5)$$

with asymptotic boundary conditions similar to a bound state. Thus one can apply bound-state techniques for its solution. We expand Ψ_0 and $\tilde{\Psi}$ in terms of the six-body symmetrized hyperspherical harmonics (HH) [5]. The expansion is performed up to maximal values of the HH grand-angular momentum quantum number K_{max}^0 for Ψ_0 and K_{max} for $\tilde{\Psi}$. We

improve the convergence of the HH expansion using the effective interaction hyperspherical harmonics (EIHH) approach [6], where the bare potential is replaced by an effective potential constructed via the Lee-Suzuki method [7]. When convergence is reached, however, the same results are obtained as with the bare potential (see Ref. [6]).

As in [1] we evaluate the LIT calculating the quantity $\langle \tilde{\Psi} | \tilde{\Psi} \rangle$ directly via the Lanczos algorithm [8]. We study the convergence of the LIT as a function of K . Our procedure consists in increasing K_{max}^0 until convergence of the ground state is reached and then studying the behavior of the LIT with growing K . In case of the AV4' potential a sufficiently convergent result for the bound state is reached with $K_{max}^0 = 12$ (yielding binding energies $E_0 = 32.90$ MeV for ${}^6\text{He}$ and $E_0 = 36.47$ MeV for ${}^6\text{Li}$). Since $\tilde{\Psi}$ depends on Ψ_0 we also check whether the norm $\langle \tilde{\Psi} | \tilde{\Psi} \rangle$, i.e. $L(\sigma_R, \sigma_I)$, converges for $K_{max}^0 = 12$. Indeed the transforms $L(\sigma_R, \sigma_I = 10 \text{ MeV})$ obtained with $K_{max}^0 = 12$ and 14 at fixed K differ by less than 1%. In case of a central S-wave interactions only, as for MTI-III [9] and MN [10] potentials, convergence is already reached at $K_{max}^0 = 10$.

In Fig. 1 we show the convergence of the LIT for ${}^6\text{Li}$ for the AV4' and the MTI-III potentials. In the upper panel the two LIT results obtained with the highest considered K_{max} are presented, while in the two lower panels we show the relative error R in percentage, for the two potentials separately. The quantity $R(\%)$ is defined as

$$R(\%) = \frac{(L(K) - L(K_{max}))}{L(K_{max})} \times 100. \quad (6)$$

One can clearly see a rather nice convergence pattern with increasing K .

In Fig. 2 we present an analogous picture for ${}^6\text{He}$ with the AV4' and the MN potentials. One finds rather satisfactory results, but compared to ${}^6\text{Li}$ the AV4' case exhibits a slower convergence, e.g., in the lower σ_R range, where mainly strength from the threshold region is sampled, one has $R(K_{max} = 11) \simeq 1\%$ in case of ${}^6\text{Li}$ and $R(K_{max} = 11) \simeq 3\%$ in case of ${}^6\text{He}$. Figures 1 and 2 also illustrate that the convergence is better for pure S-wave potentials. Thus an addition of P-wave interaction seems to lead to a slightly weaker convergence of the HH expansion. In fact performing LIT calculations with a modified AV4' potential, namely with switched off P-wave interaction, we get a convergence pattern similar to those of MN or MTI-III potentials.

In the following we want to describe in some more detail the LIT calculation with $K_{max} = 13$. In Table I we list the number N of ${}^6\text{Li}$ -HH basis states as a function of K_{max} . For the

total number of basis functions one has to multiply N by the number N_ρ of hyperradial states ($N_\rho \approx 30$). Thus the total number of states becomes quite high and it is desirable to discard HH states which give only negligible contributions to the LIT. To this end we study the importance of the HH states according to their spatial symmetries. We find that quite a few of them can be safely neglected beyond given K_{max} values (see Table II). In this way for $K_{max} = 13$ we accomplish a reduction from $N = 18402$ to $N = 6362$. As one can see in Table II, the symmetries labelled [111111],[21111] and [3111] are not included at all and others, namely [2211] and [321], are considered only up to $K_{max}^{sym} = 7$ and $K_{max}^{sym} = 11$, respectively. We have checked the quality of our approximation, performing full calculations without cuts for lower K values and comparing the obtained LIT results with those of a truncated calculation. When differences are negligible we conclude that omitted states have no influence also in calculations with higher K . The omission of the $K=13$ states of symmetry [321] could not be checked in such a way, but already its $K=11$ contribution is almost negligible and thus its $K=13$ contribution should be of no importance. In an analogous way we carry out the calculation of the LIT for ${}^6\text{He}$. We would like to mention that for this nucleus one has two separate HH expansions for $\tilde{\Psi}$, namely for the two isospin channels with $T=1$ and 2 (see also [1]).

After having discussed the convergence of the LIT we turn to the photodisintegration. In order to obtain the total photoabsorption cross section $\sigma(\omega)$ one has to invert the LIT of (4) (for details see [11]). This leads to the response function $R(\omega)$ and thus to $\sigma(\omega)$, Eq. (1).

In Fig. 3 we show the results for the total photoabsorption cross section of ${}^6\text{Li}$ and ${}^6\text{He}$ with the AV4' potential. In comparison we also present our previous results from [1] with MN and MTI-III potentials. One notes that the general structure of the cross section is similar for the various potential models, in particular the presence of two peaks for ${}^6\text{He}$, but one also finds potential dependent results for peak positions and peak heights. The double peak structure of ${}^6\text{He}$ can be interpreted as a response of a *halo* nucleus, where the low-energy peak is due to the *halo*- α core oscillation (soft dipole response) and the peak at higher energies due to the neutron-proton spheres oscillation (Gamow-Teller mode or hard dipole response).

In Fig. 4 we show the theoretical results together with available experimental data. Here we would like to mention that the data of [12] have been taken via a semi-inclusive (γ, n)

measurement. The obtained results correspond to the inclusive cross section up to an energy of about 15.7 MeV, where additional channels open up. The cross section due to those additional channels have been measured in further experiments [13, 14]. In order to have an estimate for the total cross section we have simply summed the (γ, n) data of [12] to the cross sections of [13, 14]. The data of Fig. 4 cited as [13, 14] are these sums.

Figure 4 shows that for the AV4' potential one finds an enhancement of strength in the threshold region compared to the S-wave potentials. It is evident that the inclusion of the P-wave interaction improves the agreement with experimental data considerably. This is particularly the case for ${}^6\text{Li}$. In fact with the AV4' potential one has a rather good agreement with experimental data up to about 12 MeV. In case of ${}^6\text{He}$ the increase of low-energy strength is not sufficient, there is still some discrepancy with data. Probably, in order to describe the *halo* structure of this nucleus in more detail additional potential parts are needed. In particular the spin-orbit component of the NN potential could play a role in the determination of the soft dipole resonance. In fact in a single particle picture of ${}^6\text{He}$ the two *halo* neutrons will mainly stay in a p-state and can interact with one of the core nucleons via the NN LS-force. Another reason for the discrepancy could be the convergence. As already pointed out, our HH convergence is quite satisfactory for ${}^6\text{Li}$, whereas it is still not yet fully complete in case of ${}^6\text{He}$. The pronounced *halo* structure of this nucleus could make the HH expansion more difficult. Nevertheless we would like to emphasize again that for all three potential models a typical ${}^6\text{He}$ *halo* response appears automatically from a microscopic six-body calculation, while other details of the response are very sensitive to the interaction model.

In conclusion we can say that the P-wave interaction has an important impact on the low-energy total photoabsorption cross section of the six-body nuclei. It enhances the low-energy strength quite significantly. It also leads to a considerable improvement in the comparison of theoretical and experimental results, even if a fully satisfactory agreement is not yet reached. Further investigations, both in theory and experiment, are needed. As already pointed out in [1] experimental data are too few (${}^6\text{He}$) or do not present a clear picture (${}^6\text{Li}$). On the other hand, from the theoretical point of view, more effort has to be addressed to the inclusion of additional parts in the NN potentials. Such future studies should lead to a better understanding which NN potential parts are relevant in the six-nucleon photodisintegration.

Acknowledgements

One of us (S.B.) thanks H. Arenhövel for helpful discussions. The work of N.B. was supported by the Israel Science Foundation (grant no. 202/02). A great parts of the numerical calculations were performed at the computer centre CINECA (Bologna).

-
- [1] S. Bacca, M.A. Marchisio, N. Barnea, W. Leidemann, and G. Orlandini, Phys. Rev. Lett. **89**, 052502 (2002).
 - [2] V. D. Efros, W. Leidemann, and G. Orlandini, Phys. Lett. B **408**, 1 (1997).
 - [3] R.B. Wiringa and S.C. Pieper, Phys. Rev. Lett. **89** (2002) 182501.
 - [4] V. D. Efros, W. Leidemann, and G. Orlandini, Phys. Lett. B **338**, 130 (1994).
 - [5] N. Barnea and A. Novoselsky, Ann. Phys (N.Y.) **256**, 192 (1997); Phys. Rev. A **57**, 48 (1998).
 - [6] N. Barnea, W. Leidemann, and G. Orlandini, Phys. Rev. C **61**, 054001 (2000); Nucl. Phys. **A693**, 565 (2001).
 - [7] K. Suzuki and S. Y. Lee, Prog. Theor. Phys. **64**, 2091 (1980).
 - [8] M.A. Marchisio, N. Barnea, W. Leidemann, and G. Orlandini, Few-Body Syst. in print, e-print nucl-th/0202009.
 - [9] R. A. Malfliet and J. A. Tjon, Nucl. Phys. **A127**, 161 (1969).
 - [10] D. R. Thomson, M. LeMere and Y. C. Tang, Nucl. Phys. **A286**, 53 (1977); I. Reichstein and Y. C. Tang, *ibid.* **A158**, 529 (1970).
 - [11] V.D. Efros, W. Leidemann, and G. Orlandini, Few-Body Syst. **26**, 251 (1999).
 - [12] B. L. Berman, R.L. Bramblett, J.T. Caldwell, R.R. Harvey, and S.C. Fultz, Phys. Rev. Lett. **15**, 727 (1965).
 - [13] Y. M. Shin, D.M. Skopik, and J.J. Murphy, Phys. Lett. **55B**, 297 (1975).
 - [14] G. Junghans, K. Bangert, U.E.P. Berg, R. Stock, and K. Wienhard, Z. Physik A **291**, 353 (1979).
 - [15] T. Aumann *et al.*, Phys. Rev. C **59**, 1252 (1999).
 - [16] T. Aumann (private communication).

TABLE I: Number N of ${}^6\text{Li}$ HH basis states for various K_{max} values.

K_{max}	5	7	9	11	13
N	52	323	1489	5665	18402

TABLE II: Cut of symmetries for the ${}^6\text{Li}$ calculation with $K_{max} = 13$. For a given symmetry N^{sym} denotes the number of included basis states and K_{max}^{sym} is the maximal considered value of the grand-angular momentum quantum number for this symmetry.

Symmetry	[111111]	[21111]	[2211]	[3111]	[321]	[411]	[33]
N^{sym}	0	0	50	0	2382	2598	1332
K_{max}^{sym}	–	–	7	–	11	13	13

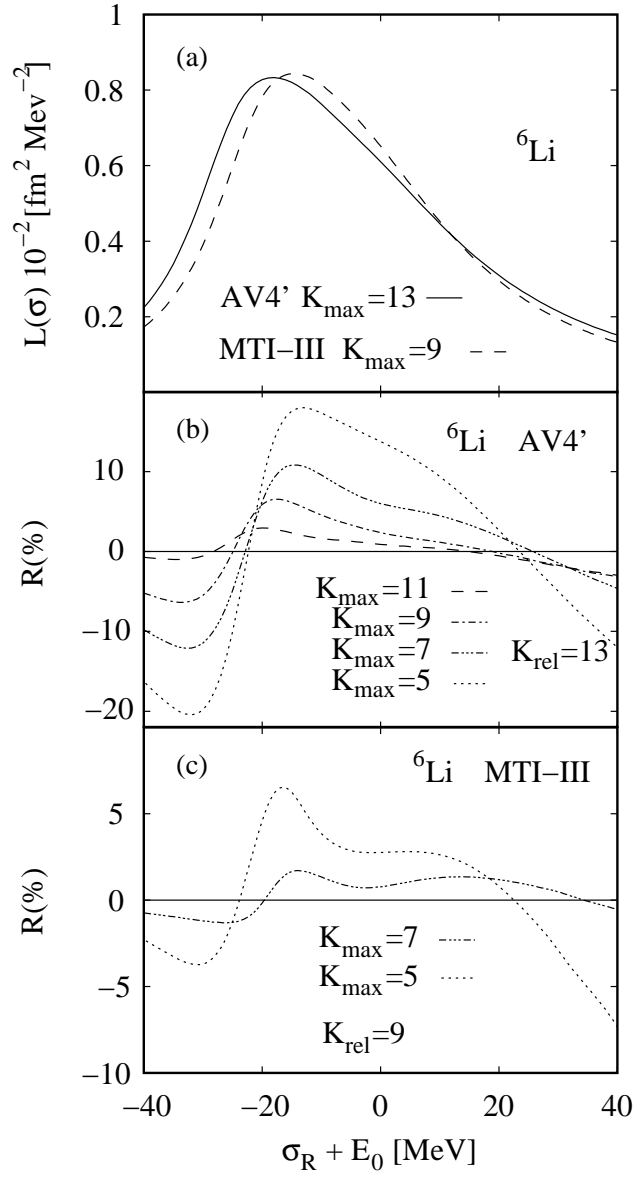


FIG. 1: (a) LIT for ${}^6\text{Li}$ ($\sigma_I = 10$ MeV) with AV4' and MTI-III potentials; HH convergence of LIT as function of K with $K_{\text{max}} = 13$ (see (6)) for AV4' (b) and MTI-III (c) potentials.

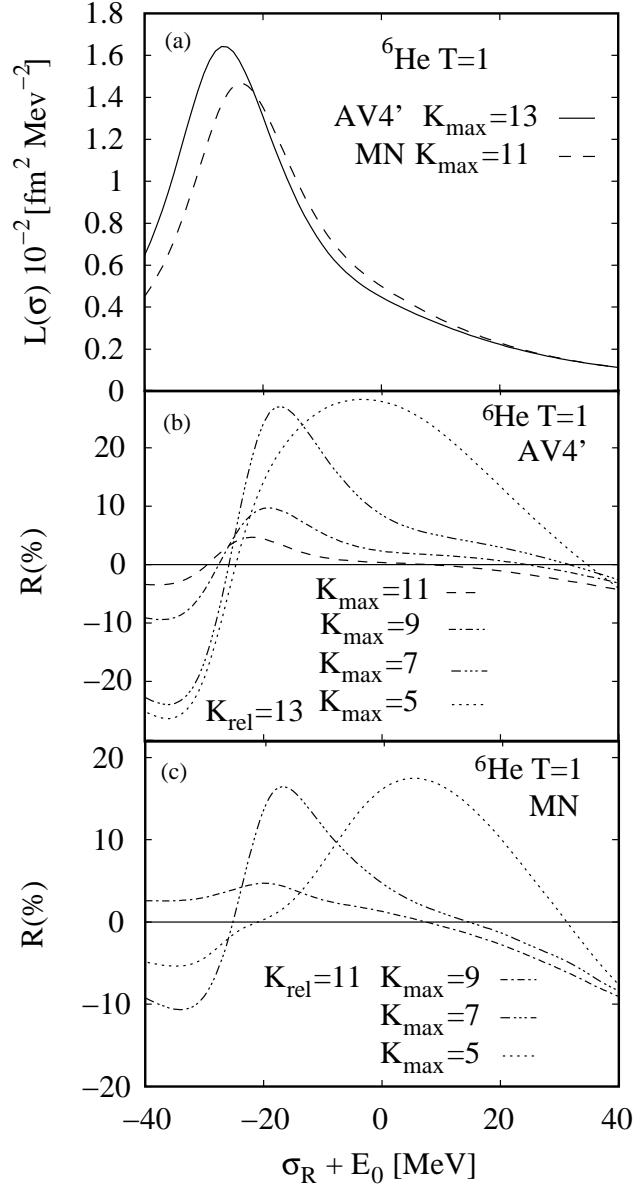


FIG. 2: (a) LIT for ${}^6\text{He}$ ($\sigma_I = 10$ MeV) with AV4' and MN potentials; HH convergence of LIT as function of K with K_{max} (see (6)) for AV4' (b) and MTI-III (c) potentials.

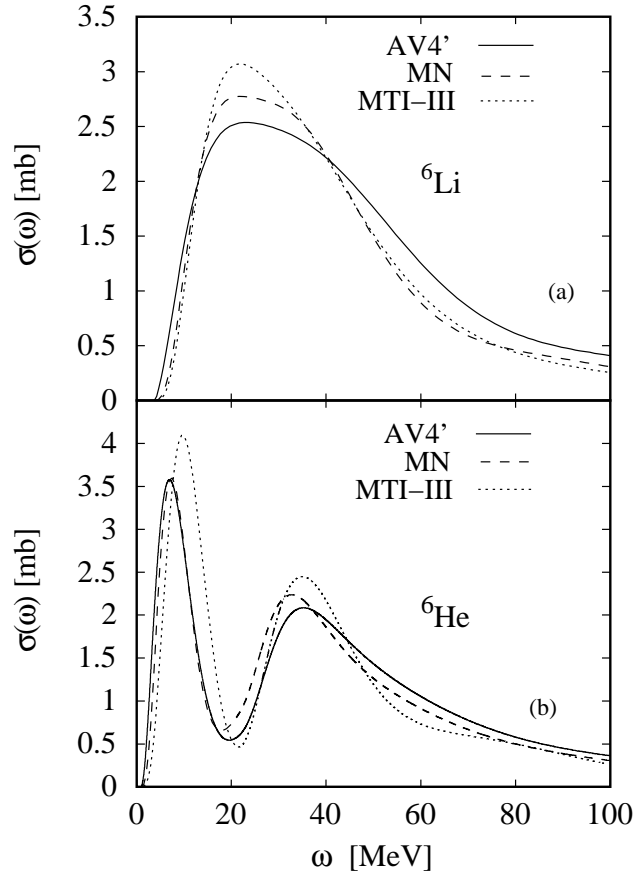


FIG. 3: Total photoabsorption cross sections for the six-body nuclei with AV4', MN and MTI-III potentials: ${}^6\text{Li}$ (a), ${}^6\text{He}$ (b).

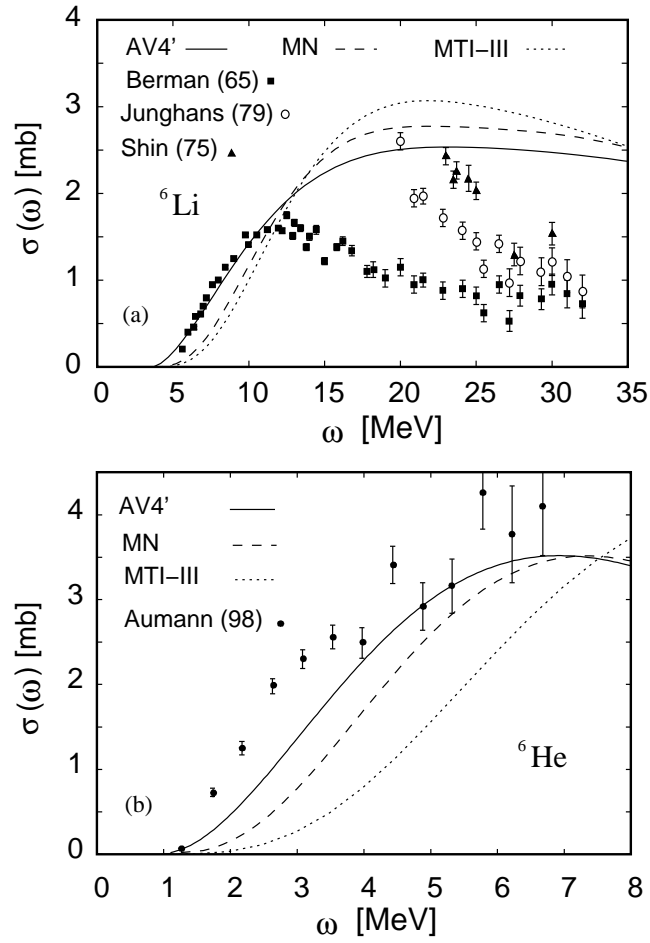


FIG. 4: Theoretical and experimental photoabsorption cross section results (see also text): (a) ${}^6\text{Li}$ with experimental data from [12, 13, 14], (b) ${}^6\text{He}$ with data from [15, 16] (theoretical results convoluted with instrumental response function).